Pressure-Tuned Spin and Charge Ordering in an Itinerant Antiferromagnet

Yejun Feng,[1] R. Jaramillo,[1] G. Srajer,[2] J. C. Lang,[2] Z. Islam,[2] M. S. Somayazulu,[3] O. G. Shpyrko,[4] J. J. Pluth,[5] H.-k. Mao,[3] E. D. Isaacs,[1,4] G. Aeppli,[6] and T. F. Rosenbaum[1,*]

[1]*The James Franck Institute and Department of Physics, The University of Chicago, Chicago, Illinois 60637, USA*
[2]*The Advanced Photon Source, Argonne National Laboratory, Argonne, Illinois 60439, USA*
[3]*Geophysical Laboratory, Carnegie Institute of Washington, Washington, D.C. 20015, USA*
[4]*Center for Nanoscale Materials, Argonne National Laboratory, Argonne, Illinois 60439, USA*
[5]*CARS and Department of Geophysical Sciences, The University of Chicago, Chicago, Illinois 60637, USA*
[6]*London Centre for Nanotechnology and Department of Physics and Astronomy, UCL, London, WC1E 6BT, United Kingdom*
(Received 10 June 2007; published 24 September 2007)

Elemental chromium orders antiferromagnetically near room temperature, but the ordering temperature can be driven to zero by applying large pressures. We combine diamond anvil cell and synchrotron x-ray diffraction techniques to measure directly the spin and charge order in the pure metal at the approach to its quantum critical point. Both spin and charge order are suppressed exponentially with pressure, well beyond the region where disorder cuts off such a simple evolution, and they maintain a harmonic scaling relationship over decades in scattering intensity. By comparing the development of the order parameter with that of the magnetic wave vector, it is possible to ascribe the destruction of antiferromagnetism to the growth in electron kinetic energy relative to the underlying magnetic exchange interaction.

Electrons carry not only charge but also spin, and how magnetic order develops in metals where charge carriers remain itinerant continues to be a central problem in both condensed matter and device physics. As technology progresses and device dimensions shrink, quantum effects become more pronounced and a variety of potential ground states can emerge with coupled charge, spin, and orbital order [1]. These effects are most acute near quantum phase transitions, where magnetism first emerges at the absolute zero of temperature [2,3]. In particular, antiferromagnetic coupling between interacting mobile electrons is believed to underlie some of the most profound puzzles in modern metal physics, most notably exotic superconductivity, heavy fermions, and other non-Fermi-liquid phenomena [4,5].

Nevertheless, definitive characterization of quantum critical behavior in itinerant magnets has proved elusive. Direct order parameter studies of stoichiometric, itinerant ferromagnets suggest that the quantum phase transition is always first order, shrouding the critical behavior [6]. Quantum critical behavior in itinerant antiferromagnets has been observed using indirect probes such as electrical transport and specific heat [5], but no direct studies of the order parameter of stoichiometric antiferromagnets exist. As a further complication, the effects of chemical doping and substitution are amplified at a quantum phase transition, where materials become "hypersensitive" to disorder [7].

Directly observing the emergence of antiferromagnetism in a model stoichiometric system without the application of a symmetry-breaking field or dopant disorder would reveal fundamental aspects about the magnetic order itself. To this end, we present a direct x-ray diffraction study of the spin and charge order parameters in elemental chromium, the archetypal itinerant spin-density-wave

(SDW) antiferromagnet, as the magnetic order is suppressed with pressure towards its quantum phase transition. Cr is attractive as a model system [8–12] and is particularly amenable to theoretical exposition given its simple bcc crystal lattice and well-understood Fermi surface, disorder-free magnetic tunability [13], and availability in high purity, single-crystal form [14].

The SDW in Cr is stabilized by two nested sheets of Fermi surface, which are eliminated in the magnetic phase by the formation of an exchange-split energy gap [8]. The SDW is modulated by a wave vector Q which is selected by the nesting condition and is slightly incommensurate with the crystal lattice [Fig. 1(a)]. Q may lie with equal probability along any of the three cubic axes, defining three orthogonal Q-domains. Below the Néel temperature, $T_N = 311$ K, and above the spin-flip temperature, $T_{SF} = 123$ K, the SDW is transverse and the spins preferentially lie along either cubic axis perpendicular to Q, defining two possible S-domains; below T_{SF} the SDW is longitudinal [16]. The SDW is accompanied by a charge density wave (CDW), which is modulated by $2Q$ and is usually thought of as the second harmonic of the SDW [10]. This harmonic relationship between spin and charge is consistent with the $I_{CDW} \propto I_{SDW}^2$ scaling (where I is scattering intensity) that is observed as a function of T [16], but has not been tested as the ground state is tuned towards the quantum critical point.

Early transport studies of the pressure P dependence of antiferromagnetism in Cr placed the $T = 0$ phase transition above 8 GPa [13], necessitating the use of a diamond anvil cell. The capability of probing the spin (SDW) and charge (CDW) order parameters using x-ray diffraction has been demonstrated previously at ambient P [16,17]. Here we extend such measurements to high P at liquid helium
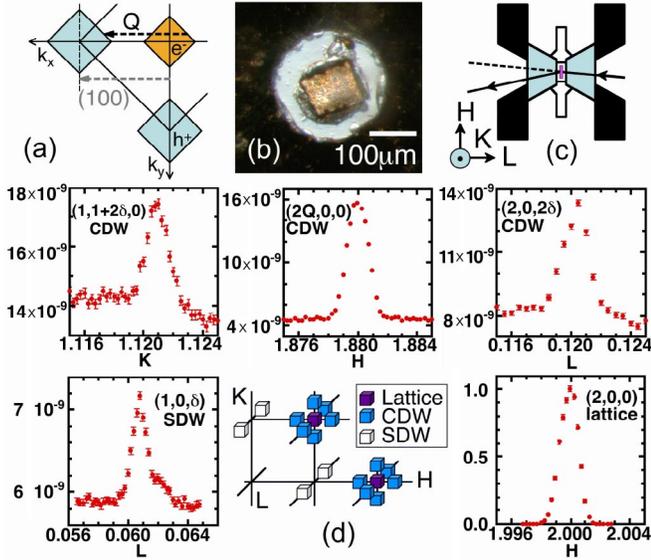
FIG. 1 (color online).   X-ray diffraction measurement of in-
commensurate SDW and CDW in a diamond anvil cell.
(a) Schematic of Cr's Brillouin zone; only the two d-like bands
involved with magnetic ordering are shown for clarity. The
nesting vector $Q = 1 - \delta$ is incommensurate with the lattice,
and depends on the relative size of the electron (orange) and hole
(light blue) octahedra. (b) Typical view through the pressure
chamber shows a single-crystal Cr sample, roughly $120 \times 100 \times 40\ \mu m^3$ in size. (c) Schematic of diffraction in the transmission
geometry through the cell. Cr crystal (purple) is prepared with
one cubic direction (e.g., L) aligned parallel to the cell axis.
(d) High-resolution and high-sensitivity monochromatic x-ray
diffraction from Cr at 8 K and 4.0 GPa. Schematic (not to scale)
shows diffraction peaks that are accessible given our cell ge-
ometry, all of which are within or very close to the H-K plane.
SDW and CDW Bragg reflections appear as satellites around
cubic reciprocal lattice points [16]. Five panels show typical raw
scans of the lattice, CDW, and SDW Bragg peaks. All data have
been normalized to the (2,0,0) peak intensity.

temperatures [Figs. 1(b) and 1(c), [14]]. Our sensitivity is
approximately 5×10^{-10} relative to the bcc Bragg inten-
sity (1/10th of the background), which is sufficient for
following the spin and charge order parameters into the
quantum critical region.

Precise measurement of the order parameters is compli-
cated by the presence of Q and S domains, all of which
must be accounted for if the SDW and CDW diffraction
intensities are to be properly normalized. By measuring
CDW peaks corresponding to all three Q-domain types
[Fig. 1(d) schematic] and taking into account the atomic
form factor [18] and the appropriate strain wave cross
section [16], we are able to calculate the Q-domain distri-
bution, presented in Fig. 2(a). The unpredictable evolution
of the domain distribution with pressure underscores the
need to account for the entire domain structure when
measuring the order parameters. Furthermore, the presence
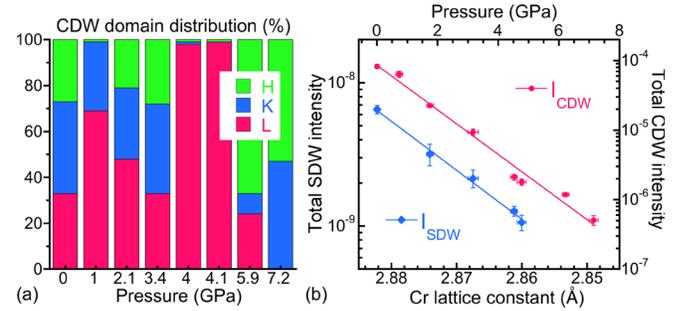of Q domains along all three cubic axes attests to the

FIG. 2 (color online).   (a) CDW Q-domain distributions for
samples at different pressures and 8 K; ambient P data were
taken at 130 K in the transverse phase to be consistent with the
high-pressure points. (b) SDW and CDW diffraction intensities
$I_{SDW} = I_{(1,0,\delta)}/I_{200}$ and $I_{CDW} = I_{(2Q,0,0)}/I_{200}$ as a function of
pressure at $T = 8$ K. Data have been normalized to the (2,0,0)
lattice Bragg peak intensity and account for Q- and S-domain
distributions. Both intensities are suppressed exponentially with
the BCS form $I_X \propto \exp(C_X \Delta a/a_0)$, where $a_0 = 2.8820$ Å is the
lattice constant at ambient P and 8 K; $C_{SDW} = 227 \pm 10$,
$C_{CDW} = 457 \pm 25$.   The $I_{CDW} \propto I_{SDW}^2$ scaling between the
CDW and SDW intensities at $T = 8$ K is consistent with scaling
seen at ambient pressure where T is varied [16].

quasihydrostatic nature of the pressure environment. A
uniaxial compressive stress along the DAC axis would
favor domains with Q along the L direction, owing to the
orthorhombic symmetry of the crystal in the SDW phase.
Even for the pressure with the most imbalanced domain
distribution (4.1 GPa), the uniaxial stress is estimated to be
less than 0.02 GPa based on the strain necessary to force a
single Q-domain state [19].

We find that the longitudinal phase is completely sup-
pressed above $P \approx 1$ GPa at $T = 8$ K, so that all high-
pressure measurements presented here are made in the
transverse phase. Therefore, it is necessary to measure
two inequivalent SDW reflections [such as $(1,0,\pm\delta)$ and
$(0,1,\pm\delta)$] in order to determine the S-domain distribution.
The SDW ordered moment is then calculated from the
equation

$$I_{SDW}/I_{Lattice} = (\hbar\omega/m_e c^2)^2 (f_m/f)^2 (\mu/N)^2, \qquad (1)$$

where $\hbar\omega$ is the x-ray energy, f_m and f are the magnetic
[17] and atomic [18] form factors, N is the number of
electrons per site, μ is the (rms) ordered moment per
atom in units of μ_B [16], and I_{SDW} and $I_{Lattice}$ are the
(properly normalized) SDW and lattice diffraction inten-
sities. Our measured ordered moment at ambient P is
$0.39 \pm 0.02 \mu_B$, consistent with the accepted value of
$\mu_0 = 0.41$ [16].
We plot in Fig. 2(b) the evolution of the SDW and CDW
diffraction intensities with P at $T = 8$ K. Both order pa-
rameters are seen to scale exponentially with pressure over
the entire measurement range. The quadratic scaling be-
tween I_{CDW} and I_{SDW} holds as a function of pressure,
indicating that the coupling of the spins to the charge is

not altered by varying the lattice constant. The exponential
dependence of the ordered magnetic moment on pressure
can be understood within the framework of the two band
model of a nested SDW, which for the case of perfect
nesting is analogous to a BCS superconductor [8]. To the
extent that the exchange potential between the two nested
sheets of Fermi surface is a constant, the model predicts
that $\mu \propto g_0$, where $2g_0$ is the energy gap responsible for
eliminating the magnetic Fermi surfaces [8]. We therefore
apply the expression for the gap [8]

$$g_0 \propto \exp(-2\pi^2 v/\gamma^2 \bar{V} k_c^2) \equiv \exp(-1/\lambda), \qquad (2)$$

to the experimentally determined ordered moment. Here γ
is an average exchange integral, $\bar{V}$ is an average Coulomb
potential, $4\pi k_c^2$ is the Fermi surface area of the magnetic
bands, and v is an average Fermi velocity. Comparing our
data to Eq. (2) we see that $1/\lambda$, the ratio of kinetic energy
density $t = v/k_c^2$ to exchange potential density $J = \gamma^2 \bar{V}$ in
reciprocal space, varies linearly with P. The exponential
decrease in ordered moment with pressure is consistent
with the similar decrease in $T_N \propto \exp(C_T \Delta a/a_0)$ with
$C_T = 93$ [13]. We conclude that the suppression of anti-
ferromagnetic order with pressure at the approach to the
quantum critical point is described simply by a BCS-like
linear relationship between T_N and g_0.

  Pressure can suppress the gap g_0 principally through
either the magnetic exchange coupling or the Fermi surface
geometry of the magnetic bands. We separate these effects
by studying the P dependence of the SDW wave vector Q,
which reflects the evolution of the band structure and the
nesting condition. We compare in Fig. 3(a) the P depen-
dence of Q at low T and its T dependence at ambient P.
$Q(P)$ appears to flatten off with increased pressure, ap-
proaching a constant for $P > 4$ GPa. Given that the ob-
served exponential dependence of μ on P continues to at
least 7.2 GPa, this demonstrates that the change in Q is not
directly related to the evolution of $g_0 \propto \exp(-1/\lambda)$.
Changes in Q at $T = 0$ reflect changes in the geometry
of the underlying paramagnetic nested Fermi surfaces,
resulting from a redistribution of electrons in reciprocal
space; for a rigid band structure Q would remain constant
with pressure. The data show that the geometry of the
nesting bands is essentially pressure independent, ap-
proaching the rigid limit for $\Delta a/a_0 > 1\%$.

  It is important to consider the possibility that imperfect
nesting may alter the physics. In such a case, the spin
response function at $\chi_0(q = Q)$ would exhibit a broad
maximum rather than a singular cusp [20], and g would
be renormalized away from g_0 [9]. However, this posited
renormalization is inconsistent with the observed exponen-
tial decrease in g with pressure, indicating that the giga-
Pascal pressures applied in our experiment do not warp the
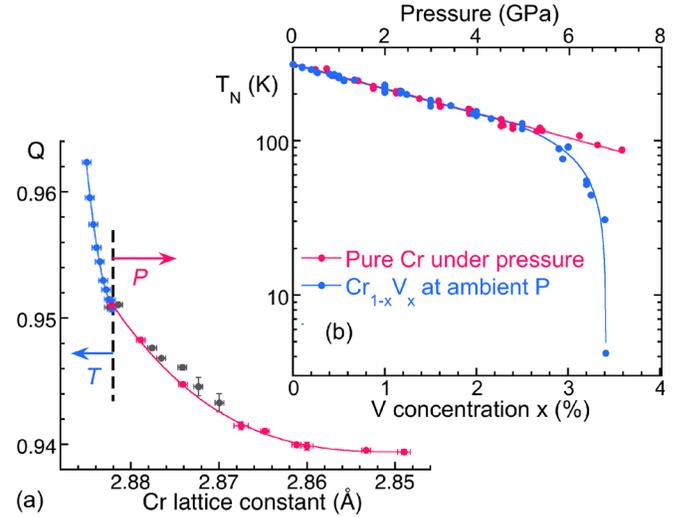band structure to the extent of significantly affecting the
nesting condition.

FIG. 3 (color online).   (a) Evolution of the SDW wave vector Q
[in units of $2\pi/a(P)$] with temperature and pressure. Q becomes
independent of P at the approach to the quantum phase tran-
sition. T dependence at ambient P (blue) and P dependence at
92 K (gray) were measured with energy dispersive x-ray diffrac-
tion [15]; P dependence at 8 K (red) was measured with a
monochromatic technique. Solid lines are guides to the eye.
(b) Pressure (red) and vanadium doping (blue) track until dis-
order disrupts the BCS behavior. T_N for pure Cr under pressure is
derived by using a linear relationship $T_N(P) = \mu(P)/\mu_0 \times$
311 K, and from Ref. [13] with a pressure scale reduced by a
factor of 1.24 to account for the difference in pressure calibra-
tions. T_N for $Cr_{1-x}V_x$ are collected from Refs. [11,12,21,22] and
Refs. [15–17] within [12] for dopant concentrations up to $x_c =$
3.42%. The conversion between P and x is set by the collapse of
all the doping data for $x \leq 2.5\%$ onto the same exponential
curve of pure Cr data under pressure, giving $dP/dx =$
1.99 GPa/%.

  The contrast between the physics of clean and disor-
dered materials is brought into sharp relief in Fig. 3(b). It is
possible to suppress T_N not only with pressure, but also by
doping with V [11,21]. The two techniques track over a
wide range, but chemical doping, which introduces both
disorder and change in the average electron count, drives
the system away from a BCS form for $T_N \leq 2/5 T_N(x =$
0, $P = 0)$. The simple description of the evolution of mag-
netism in terms of the BCS energy gap is cut off by
disorder, hastening the onset of the proximate quantum
phase transition. Furthermore, for 2.5% V doping ($T_N \approx$
125 K) the low-T value of Q moves to 0.922 and μ is
suppressed to $0.24\mu_0$ [22]. By comparison, compressing
pure Cr drives μ to $0.24\mu_0$ when $Q = 0.9394$, only 1/3 the
change in Q. The evolution of $Q(x)$ for $Cr_{1-x}V_x$ [22,23]
does not level off for larger values of x as does $Q(P)$.
Therefore, we find that chemical doping in the form of
deviations from stoichiometry alters Cr's band structure to
considerably larger degree than applying pressure. At a
minimum this makes separating competing physical ef-
fects more difficult and at a maximum may point to the

PHYSICAL REVIEW LETTERS

mechanism by which deviations from pure BCS-like behavior ensue.

The direct measurement of the SDW and CDW order parameters at temperatures where thermal fluctuations are frozen out, combined with the flattening off of the SDW wave vector at the approach to the quantum critical point, reveal that it is the ratio of magnetic exchange to kinetic energy, $\lambda = J/t$, which drives the quantum phase transition in pure Cr. A quantitative estimate for λ can be obtained from recalling that for three-dimensional Fermi liquids we expect the total kinetic energy of the electrons to scale like a^{-5}, which increases strongly under pressure as a quantum confinement effect. From the data up to $P = 7.2$ GPa, the fractional change in the kinetic energy $\Delta t/t_0 = -5\Delta a/a_0 = 0.06$ which, together with the measured $\Delta(1/\lambda) = 1.3$, leads to $\lambda = J/t \sim 0.05$. We have assumed that the exchange interactions are not sensitive to the lattice constant, and indeed, if anything, they should become stronger with pressure, which would imply an even larger kinetic energy contribution to the change in λ. In this picture, the magnetic order is destabilized by the increase in the kinetic energy due to quantum confinement.

Even with λ small, the spin interactions can be robust. Inelastic neutron scattering studies demonstrate that spin-spin correlations survive up to surprisingly high energies and temperatures [24], and the Hall coefficient retains a strong temperature dependence well above the Néel transition [11]. The intrinsic exchange-driven pairing potential is thus strong in Cr, but its ground state evolution still can be modeled by the BCS-like gap solution given the high density of carriers and consequent high degree of pair overlap [25]. Of course, the BCS form for the order parameter only approaches zero asymptotically. As with chemical doping [Fig. 3(b)], the curve is likely to turn over and assume a critical form at sufficiently large P. Alternate broken symmetries such as superconductivity become a possibility if disorder is sufficiently weak, as does the survival of a purely second-order quantum phase transition, depending on the strength of the coupling of the harmonics to the primary SDW [10].

In summary, we have performed a direct study of spin and charge ordering in the stoichiometric itinerant antiferromagnet Cr as the magnetic order is suppressed with pressure. We find that this suppression is an effect of quantum confinement, the ground state evolves in accordance with the BCS weak-coupling theory, and the spin and charge degrees of freedom have a persistent harmonic relationship. The low-T behavior of the pure element differs dramatically from that of the family of doped systems approaching the quantum phase transition.

*Corresponding author.
tfr@uchicago.edu
 [1] E. Dagotto, Science **309**, 257 (2005).
 [2] A. J. Millis, Phys. Rev. B **48**, 7183 (1993).
 [3] S. Sachdev, Science **288**, 475 (2000).
 [4] N. D. Mathur *et al.*, Nature (London) **394**, 39 (1998).
 [5] J. Custers *et al.*, Nature (London) **424**, 524 (2003).
 [6] C. Pfleiderer, J. Phys. Condens. Matter **17**, S987 (2005).
 [7] P. Coleman *et al.*, J. Phys. Condens. Matter **13**, R723 (2001).
 [8] A. W. Overhauser, Phys. Rev. **128**, 1437 (1962); P. A. Fedders and P. C. Martin, Phys. Rev. **143**, 245 (1966).
 [9] T. M. Rice, Phys. Rev. B **2**, 3619 (1970).
[10] C. Y. Young and J. B. Sokoloff, J. Phys. F **4**, 1304 (1974).
[11] A. Yeh *et al.*, Nature (London) **419**, 459 (2002).
[12] M. Lee *et al.*, Phys. Rev. Lett. **92**, 187201 (2004).
[13] D. B. McWhan and T. M. Rice, Phys. Rev. Lett. **19**, 846 (1967).
[14] Miniature Cr single-crystals with a FWHM mosaicity varying from 0.05° to 0.18° were prepared from a large single-crystal wafer (Alfa Aesar, 99.996 + %) following procedures in Ref. [15]. A methanol/ethanol (4:1) mixture was used as the pressure medium. Gold was used as manometer *in situ* with an uncertainty of 0.2 GPa. Energy dispersive x-ray diffraction was performed at the bending magnet beam line 16-BM-B of the Advanced Photon Source (APS), using a chemical-filter technique to resolve the CDW peak from the adjacent lattice peak [15]. High-resolution monochromatic x-ray diffraction was performed with focused 20-keV x rays at the undulator beam line 4-ID-D at the APS.
[15] Y. Feng *et al.*, Rev. Sci. Instrum. **76**, 063913 (2005).
[16] J. P. Hill, G. Helgesen, and D. Gibbs, Phys. Rev. B **51**, 10 336 (1995).
[17] J. Strempfer *et al.*, Eur. Phys. J. B **14**, 63 (2000).
[18] M. Diana and G. Mazzone, Phys. Rev. B **5**, 3832 (1972).
[19] M. O. Steinitz *et al.*, Phys. Rev. Lett. **23**, 979 (1969).
[20] C. G. Windsor, J. Phys. F **2**, 742 (1972).
[21] M. A. Taylor, J. Less-Common Met. **4**, 476 (1962); A. S. Barker, Jr. and J. A. Ditzenberger, Phys. Rev. B **1**, 4378 (1970); J. Takeuchi, H. Sasakura, and Y. Masuda, J. Phys. Soc. Jpn. **49**, 508 (1980); D. R. Noakes, T. M. Holden, and E. Fawcett, J. Appl. Phys. **67**, 5262 (1990); A. J. A. de Oliveira *et al.*, J. Phys. Condens. Matter **8**, L403 (1996); A. J. A. de Oliveira, W. A. Ortiz, P. C. de Camargo, and C. Yu Galkin, J. Magn. Magn. Mater. **152**, 86 (1996); D. R. Noakes, E. Fawcett, and T. M. Holden, Phys. Rev. B **55**, 12 504 (1997).
[22] W. C. Koehler, R. M. Moon, A. L. Trego, and A. R. Mackintosh, Phys. Rev. **151**, 405 (1966).
[23] E. Fawcett *et al.*, Phys. Rev. Lett. **61**, 558 (1988).
[24] S. M. Hayden *et al.*, Phys. Rev. Lett. **84**, 999 (2000); B. H. Grier, G. Shirane, and S. A. Werner, Phys. Rev. B **31**, 2892 (1985).
[25] P. Nozière and S. Schmitt-Rink, J. Low Temp. Phys. **59**, 195 (1985).